

Towards a first-principles simulation and current-voltage characteristic of atomistic metal-oxide–semiconductor structures

Alexander A. Demkov*

Physical Sciences Research Labs, Motorola, Inc., Tempe, Arizona 85284

Xiaodong Zhang and D. A. Drabold

Department of Physics and Astronomy, Ohio University, Athens, Ohio 45701

(Received 15 May 2001; published 6 September 2001)

We describe a theoretical approach to transport and a potentially valuable scheme for screening gate dielectric materials. Realistic structural models of the Si-dielectric interface are employed for Si-SiO₂-Si model metal-oxide–semiconductor (MOS) structures. The leakage current for a 1.02-nm MOS structure is calculated from first principles using Landauer’s ballistic transport approach and *ab initio* molecular-dynamic simulation. The calculated leakage currents agree with most recent experimental data.

DOI: 10.1103/PhysRevB.64.125306

PACS number(s): 73.40.Qv

The *International Technology Road Map for Semiconductors* predicts that the strategy of scaling of complimentary metal-oxide–semiconductor (CMOS) devices will come to an abrupt end around the year 2012.¹ The principal reason for this will be unacceptable leakage current through the silicon dioxide gate for a thickness below 4 nm: the insulation of the oxide layer breaks down for a very thin layer.² The looming demise of SiO₂ as a gate insulator has spurred an urgent search for an alternative gate dielectric.^{3–5} Finding such a material has proven to be far from trivial. Theoretical modeling of the low bias gate leakage current, and how it is affected by the atomic structure and chemical composition would be valuable to screen possible candidate materials.

In this paper we present a methodology that may be used to assist the materials research effort. Using a theoretical atomic level Si-SiO₂ model system we investigate the leakage current through an ultrathin metal-oxide–semiconductor (MOS) structure using the quantum transmission probability. The leakage current for a 1.9-nm MOS structure with a 1.02-nm tunneling barrier correctly reproduces the recent experimental data.⁶ A combination of the density-functional quantum molecular dynamics (QMD) and ballistic transport theory is employed.

We now discuss our approach to the leakage current calculations in nanodevices such as ultrathin MOS structures, where direct and trap assistant tunneling are primary leakage mechanisms.⁷ At the few nanometer length scale we can employ simple ballistic transport theory,⁸ and the current calculation is reduced to an effective one-dimensional potential barrier scattering problem.⁹ A ballistic description is justified for systems with dimensions below the physically important scattering lengths such as the Fermi length, mean free path, and the phase relaxation length, which in a typical semiconductor are 10 nm, 30 μm, and 1 μm, respectively. The ballistic transport through SiO₂ has been studied theoretically¹¹ and experimentally,¹² and the mean free path is reported to be between 0.6 and 1.5 nm. Since the gate oxide layer in the advanced transistor is about five atoms thick,² one can comfortably use Landauer’s formalism.

The current is given by⁹

$$I = \frac{e}{\pi\hbar} \int_{\mu_l}^{\mu_r} T(E) dE, \quad (1)$$

where

$$\mu_l = E_f - \eta eV$$

$$\mu_r = E_f + (1 - \eta) eV. \quad (2)$$

$T(E)$ is the transmission probability for electron of energy E , η describes the electrostatic potential difference, and V is divided between the two contacts. We use the $\eta = 0.5$ suggested by Datta *et al.*¹⁰

Thus the central problem is to calculate the barrier transmission function $T(E)$. The transmission probability is often calculated within the WKB approximation, or using a real-space discretization of the effective-mass Hamiltonian.⁷ Choosing a proper effective mass, however, is difficult. A wide range of values for the “tunneling” mass is used in the literature,^{13,14} and amounts to a simple fitting. The small parameter in the Luttinger-Kohn theory allowing the use of the envelope function and the effective mass itself is of the order of $(a/a_i)^2$, where a is the lattice constant, and the a_i is the extent of the “defect” state,¹⁵ which in our case is the thickness of the dielectric layer. When the thickness of the gate dielectric (the scatterer) is only 1 nm the effective-mass approximation fails (the lattice constant of Si is 5.43 Å) and necessitates an atomistic approach. Current *ab initio* electronic structure methods allow one to perform predictive calculations for systems containing hundreds and (in favorable circumstances) even thousands of atoms. This implies the nanometer length scale sought here. We propose to use the microscopic density-functional theory Hamiltonian with scattering theory to describe the low bias leakage current through the MOS structure.

To realize our program we need (i) an atomistic model of a MOS structure and (ii) a Hamiltonian to use for the transmission function calculation. We generate both using a local orbital first-principles quantum molecular-dynamics (QMD) method designed for applications to large systems and implemented in the Fireball package.^{16,17} Integrals over the Brill-

lounin zone are evaluated using the special k points of Monkhorst and Pack.¹⁸ Recent applications of the technique to materials problems are reviewed in Ref. 19. The efficacy of the approach for transport problems is suggested from applying the “reference energy method” in which we estimated the valence-band discontinuity at the Si-SiO₂ interface to be 4.67 eV,²⁰ in agreement with the recent data.²¹ As another preliminary to using the Fireball Hamiltonian for transport, we computed the effective masses for bulk Si. We find (in units of m_o) m_t , m_l , m_{hh} , and m_{lh} to be 1.015, 0.199, 0.24, and 0.163, respectively, in good agreement with experiment (0.98, 0.191, 0.537, and 0.153).²² The discrepancy in the heavy hole mass is due to the neglect of the spin-orbit interaction, which causes the band to “flatten” when the degeneracy is lifted.

We have constructed several model MOS structures. As a starting point we use models of the Si-SiO₂ interface generated by the “direct oxidation” method described in Ref. 20. Briefly, the structure consists of a silicon slab with an oxide layer “grown” on it in a QMD simulation. Si layers are separated from the stoichiometric oxide by approximately 4 Å of suboxide. Structural models of that type are used in calculations of the band offset at the interface. We constructed several cells of various dimensions and thicknesses, with and without dangling bonds at the interface. Then, in the simplest case, a mirror image of the cell is generated, and the two are fused together. That procedure results in a Si-SiO_x-SiO₂-SiO_x-Si structure. Some special care needs to be taken of the SiO₂ bonding pattern in the plane of contact. Mixing and matching the initial Si-SiO₂ structures, both symmetric and asymmetric MOS models could be built. The structure then is annealed in a high-temperature QMD run followed by a quench to a local-energy minimum. MOS model structures thus generated are used as scattering regions or “defects.” In particular we will describe the tunneling through a defect with the oxide thickness of 10.2 Å and a 5.43×5.43-Å cross section. The relaxed structure of this simulated MOS capacitor is shown in Fig. 1. There are no dangling bonds in the model. Once we have a defect model, two perfect Si regions with the same cross section as the defect, representing the leads, are considered attached on both sides of the tunneling structure. Thus the total length of the system is taken to infinity. The right Si region represents the channel, and the left region a grain of poly-Si (gate electrode).

We adopt the approach of Fisher and Lee,²³ and relate the transmission function to the Green’s function of the scattering region embedded between two semi-infinite perfect regions. Starting with the Lippman-Schwinger equation we arrive at the following expression for the transmission function $T(E)$:

$$T(E) = \text{Tr}[\hat{\Gamma}_l \hat{G}_d \hat{\Gamma}_r \hat{G}_d^+]. \quad (3)$$

Here \hat{G}_d^+ is the Green’s function of the scattering region coupled to the semiinfinite leads (l, r), and $\hat{\Gamma}_i$ is $\hat{\tau}_{di} \hat{\Delta}_i \hat{\tau}_{di}$. Operators $\hat{\tau}_{di}$ describe the coupling of the defect region to the leads. Note that the spectral density $\hat{\Delta}_i$, related to a

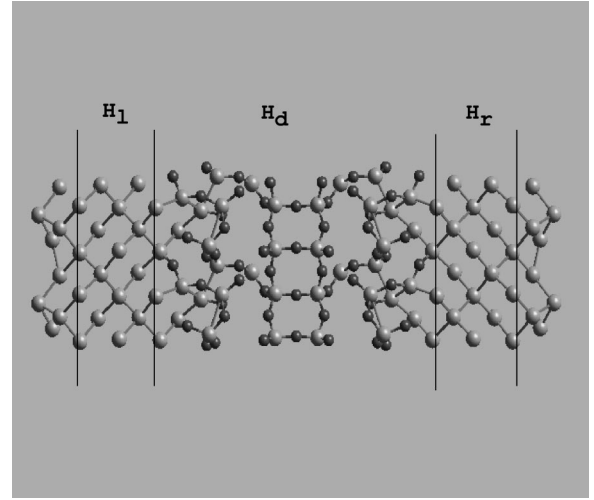


FIG. 1. A simulated MOS structure. The thickness of the oxide region is 19.00 Å including 10.2 Å of the stoichiometric SiO₂. Vertical lines indicate the portions of the structure used to compute the defect Hamiltonian H_d and its couplings to the leads.

lead’s Green’s function, rather than a band-structure derived velocity operator appears in our formalism. We have extended this approach to a nonorthogonal basis.

A salient feature in our approach is that we include several layers of the lead material in the “defect structure” as shown in Fig. 1. The coupling between the left and right leads with the oxide is then obtained directly, and is essentially exact. In principle, if we include an infinite layer of silicon at the left and right, we model the real device. The advantage of using the local orbital real-space Hamiltonian, is in that the defect denoted by the H_d in Fig. 1 interacts only with a finite (a four-layer) block of the left H_l and right H_r leads. We only assume that the orbitals of two leads are mutually orthogonal. The intralead interactions $\hat{\tau}_{ii}$ are generated exactly in separate calculations for lead structures. The Green’s functions of the semi-infinite leads used to determine $\hat{\Delta}_i$ are obtained by the iterative block recursion. The periodic boundary conditions are applied in two lateral directions. The detailed description of our approach will be published elsewhere.

The major difficulty in using an atomistic approach to the leakage current simulation is the band bending at the semiconductor-oxide interface. The characteristic dimension of the bending, the Debye length, is a function of doping and typically is on the order of a micron. This is clearly beyond the present capabilities of the most ambitious electronic structure method. To avoid this difficulty, and since we are interested in the microscopic aspects of the leakage, we consider the oxide sandwiched between two degenerate (and therefore metallic) semiconductors. Accordingly, we place the Fermi level at the edge of the Si conduction band. To determine the Fermi-level position in our sample we plot the spatial dependence of the expectation value of the Hamiltonian calculated for the valence 3s state of Si as shown in Fig. 2(a). The top of the valence band across the MOS capacitor is placed with respect to this reference level as described in Ref. 20. The band gap of Si in our technique is

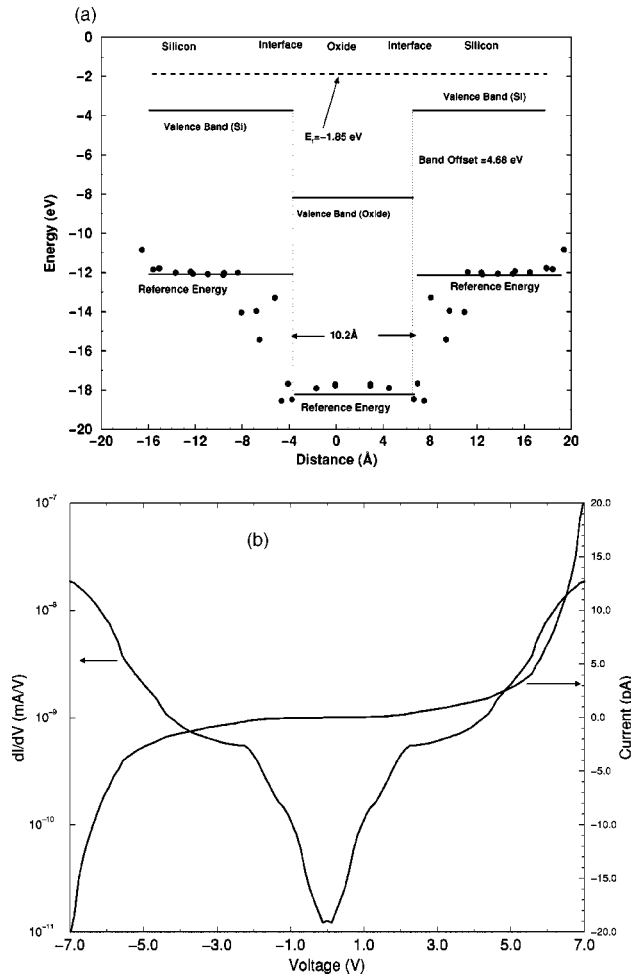


FIG. 2. (a) The Si 3s valence state matrix element plotted across the model capacitor structure shown in Fig. 1. There are no dangling bonds at the Si-oxide interface in the model. Used as a reference energy this level allows us to find the top of the valence band (Ref. 20). From the computed valence-band top of Si we place the Si Fermi level at -1.85 eV to achieve the degeneracy. The thickness of the tunneling barrier of 10.2 Å is determined by the stoichiometric oxide region marked by the energy level at -19 eV. (b) The calculated tunneling I - V characteristic of the simulated MOS structure.

1.85 eV, that puts the Fermi level at -1.85 eV. In addition, Fig. 2(a) reveals a very important feature. Notice that the perfect Si slabs of the structure are separated by 20 Å, however, the stoichiometric oxide (and the tunneling barrier) occupies a much more narrow region from -4 to 6 Å. The energy level at -19 eV corresponds to the Si oxidation state $4+$ and marks the region of a proper oxide. The calculated I - V characteristics of the simulated MOS structure are shown in Fig. 2(b). Following Datta *et al.*¹⁰ we use a simplified treatment of electrostatics, and assume the potential in the oxide varies linearly. A positive bias is applied at the left lead, and we keep the energy levels of the defect as a fixed reference, and let the leads float up and down by $V/2$. This approximation is justified for a low applied voltage because the band gap of the oxide is very large, and a small bias will cause only a very small charge transfer. In the low bias re-

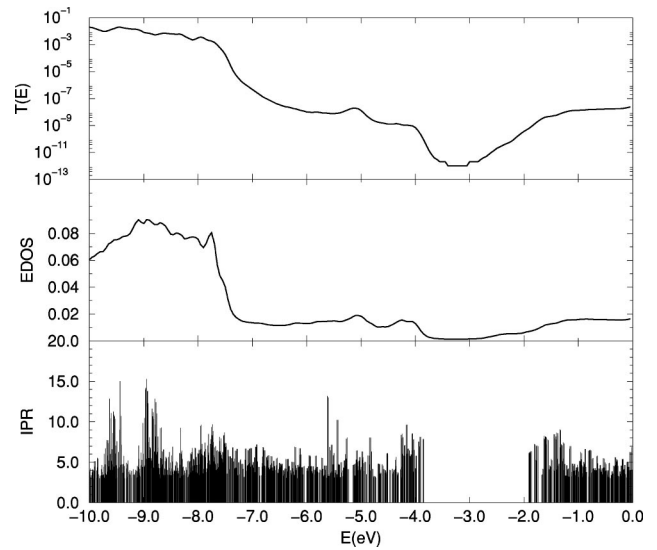


FIG. 3. The transmission functions, local density of states, and inverse participation ratio for the simulated MOS structure.

gime the current is pure tunneling across the gap of the oxide. As the voltage increases over the gap of Si the conduction band of the left lead comes in resonance with the valence band of the right lead, and the interband tunneling switches on as can be seen by a feature in the differential conductance at ~ 2.0 V. The conduction band of the oxide comes in resonance with the right lead at about 6 V and a dramatic current increase can be seen in Fig. 2.

As we will show, this behavior is easily understood from the local density of states, inverse participation ratio and transmission function of the device shown in Fig. 3. Our goal is to see how the structure of the interface translates into the transport properties. There are three distinct types of defects possible in our structures: suboxide SiO_x region where the oxidation state of Si gradually changes from 0 to $+4$, oxidation induced strain, and interfacial defects such as dangling bonds.

Our simulated MOS device does not have any dangling bonds, and the gap region from -2 eV to -4 eV is rather clean (Fig. 3). In the suboxide layer, a Si atom bonded to three Si neighbors and one oxygen produces a localized state in the valence band at -4.2 eV as well as a state at -1.6 eV in the conduction band. The “suboxide” states dominate the valence-band edge. Deeper into the band, at -5.6 eV we see localized states induced purely by the oxidation strain causing a distortion of the Si bonding near the interface. Both features produce peaks in the transmission function and in the derivative dI/dV in Fig. 2(b). The structure in dI/dV is therefore related to the weakly localized states arising from chemical and structural disorder at the interface.²⁴

The leakage currents for MOS structures with the thickness ranging from 4 to 32 Å have been recently measured at Bell Labs.⁶ The leakage current densities for a 35 -nm transistor structure with the oxide thickness of 10.2 and 19.0 Å are 19 and 10^{-3} A/cm², respectively. To emphasize the problem of the effective-mass approach we fitted the experimental data with the WKB formula and obtained m^*

$=0.95m_0$ for a thinner oxide, and $m^*=0.87m_0$ for a thicker one. Using the cross sectional area of 29.5 \AA^2 and the current of $9.84 \times 10^{-2} \text{ pA}$ at a 1-V bias [Fig. 2(b)] our theory predicts the current density of 33.2 A/cm^2 for a 10.2-\AA barrier structure (19.0 \AA total oxide thickness) in remarkable agreement with experiment. The comparison with the experiment should be done with caution, however, since the data is obtained in the inversion regime, which we approximate with the degenerate (metallic) leads. Most importantly, our technique provides a direct relationship between the features in the I - V characteristic and the microscopic nature of the device. A typical quantum-mechanical calculation includes a self-consistent solution of the Schrödinger and Poisson equations in one dimension to generate the scattering potential barrier, followed by the transmission calculation.²⁵ The transmission can be calculated with a variety of methods ranging from a simple WKB approximation¹³ to a nonequilibrium Green function approach.²⁶ As we have stated earlier, the effective-mass approximation, the band picture, and thus the potential barrier description itself are not appropriate for systems of just a few unit cells in size. This also is readily seen in Fig. 2(a). Our approach describes the electron propagation in a real material through the atomic quantum states, within a simple but sufficiently robust transport model. The method is truly three dimensional (3D). We perform a full 2D Brillouin-zone integration and thus capture the off-zone current flow.²⁷ Here we investigate the most fundamental tun-

neling structure, but we have also applied this technique to alternative gate dielectrics.²⁸ The use of quantum molecular dynamics enables us to generate realistic atomic level models^{20,29} that then are used in transport simulations. As we have shown, in a nanodevice the small deviation in the atomic arrangements at the interface (or in the dopant distribution²⁸) have a dramatic effect on the electron transport. To capture these effects one has to go to the atomic limit.

In summary, we have described a theoretical approach suitable for screening of potential gate dielectrics, studying the sub- $0.1\text{-}\mu\text{m}$ nanodevices, and to guide the experimental effort. Using a combination of the density-functional quantum molecular dynamics and ballistic transport theory we generate ultrathin MOS structures and investigate the leakage current through them. We are able to relate the microscopic atomic structure and chemistry of such a device to its transport properties accessible experimentally. This is an important step in our understanding of the nanoscale electronics.

It is our pleasure to thank D. Vasileska, R. Akis, D. Ferry, Heather Loechelt, J. Hallmark, K. Eisenbeiser, A. Talin, O. Sankey, and E. Hall for stimulating discussions and support of our work. X. Zhang thanks Motorola, Inc. for support through the Motorola Summer Internship Program.

*Email address: alex.demkov@motorola.com

¹1999 *International Technology Road Map for Semiconductors* (Industry Semiconductor Association, San Jose, 1999).

²D.A. Muller, T. Sorsch, S. Moccio, F.H. Baumann, K. Evans-Lutterdodt, and G. Timp, *Nature (London)* **399**, 758 (1999).

³R.A. McKee, F.J. Walker, and M.F. Chisholm, *Phys. Rev. Lett.* **81**, 3014 (1998).

⁴K. Eisenbeiser, J. Finder, Z. Yu, J. Ramdani, J. Curless, J. Hallmark, R. Droopad, W. Ooms, L. Salem, S. Bradshaw, and C.D. Overgaard, *Appl. Phys. Lett.* **76**, 1324 (2000).

⁵M. Copel, M. Gribelyuk, and E. Gusev, *Appl. Phys. Lett.* **76**, 436 (2000).

⁶M.L. Green, T.W. Sorsch, G.L. Timp, D.A. Muller, B.E. Weir, P.J. Silverman, S.V. Moccio, and Y.O. Kim, *Microelectron. Eng.* **48**, 25 (1999).

⁷D.Z.-Y. Ting, *Appl. Phys. Lett.* **73**, 2769 (1998).

⁸R. Landauer, *IBM J. Res. Dev.* **1**, 223 (1957).

⁹S. Datta, *Electronic Transport in Mesoscopic Systems* (Cambridge University Press, Cambridge, 1995).

¹⁰W. Tian and S. Datta, *J. Chem. Phys.* **109**, 2974 (1998); Y. Xue and S. Datta, *Phys. Rev. Lett.* **83**, 4844 (1999); S. Datta *et al.*, *ibid.* **79**, 2530 (1997); M.P. Samanta *et al.*, *Phys. Rev. B* **53**, R7626 (1996).

¹¹W. Porod and D.K. Ferry, *Phys. Rev. Lett.* **54**, 1189 (1985).

¹²D.J. DiMaria, M.V. Fischetti, J. Batey, L. Dory, E. Tierney, and J. Stasiak, *Phys. Rev. Lett.* **57**, 3213 (1986).

¹³A. Shanware, H.Z. Massoud, E. Vogel, K. Henson, J.R. Houser, and J.J. Wortman, *Microelectron. Eng.* **48**, 295 (1999).

¹⁴G. Lucovsky *et al.*, *J. Appl. Phys.* **83**, 2327 (1998).

¹⁵J.M. Luttinger and W. Kohn, *Phys. Rev.* **97**, 869 (1955).

¹⁶A.A. Demkov, J. Ortega, O.F. Sankey, and M.P. Grumbach, *Phys. Rev. B* **52**, 1618 (1995).

¹⁷O.F. Sankey and D.J. Niklewski, *Phys. Rev. B* **40**, 3979 (1989).

¹⁸H.J. Monkhorst and J.D. Pack, *Phys. Rev. B* **13**, 5188 (1976).

¹⁹O.F. Sankey, A.A. Demkov, W. Windl, J.H. Fritsch, J.P. Lewis, and M. Fuentes-Cabrera, *Int. J. Quantum Chem.* **69**, 327 (1998).

²⁰A.A. Demkov and O.F. Sankey, *Phys. Rev. Lett.* **83**, 2038 (1999).

²¹J.W. Keister, J.E. Rowe, J.J. Lolodziej, H. Niimi, T.E. Madey, and G. Lucovsky, *J. Vac. Sci. Technol. B* **17**, 1831 (1999).

²²O. Madelung, *Semiconductors-Basic Data* (Springer, New York, 1996).

²³D.S. Fisher and P.A. Lee, *Phys. Rev. B* **23**, 6851 (1981).

²⁴J. Dong and D.A. Drabold, *Phys. Rev. Lett.* **80**, 1928 (1998).

²⁵D.K. Ferry and S.M. Goodnick, *Transport in Nanostructures* (Cambridge University Press, Cambridge, England, 1997).

²⁶R. Lake, G. Klimeck, R.C. Bowen, and D. Jovanovic, *J. Appl. Phys.* **81**, 7845 (1997).

²⁷G. Klimeck, R.C. Bowen, and T.B. Boykin, *Superlattices Microstruct.* **29**, 187 (2001).

²⁸A.A. Demkov, R. Liu, X. Zhang, and H. Loehcelt, *J. Vac. Sci. Technol. B* **18**, 2388 (2000).

²⁹A.A. Korkin, A.A. Demkov, N. Tanpipat, and J. Andzelm, *J. Chem. Phys.* **113**, 8237 (2000).